Bioscene

Bioscene
Volume- 22 Number- 02
ISSN: 1539-2422 (P) 2055-1583 (O)
www.explorebioscene.com

Anti-Cancer Properties of Scutellare in cellular and in Silico Studies in Hepato cellular Carcinoma

BK Manjunatha[1], Aishwarya shivaji bagayi[1], Chaitra L[1], Deeksh G[1], Anuvarshini JM[1], Vidya SM, Syed Murthuza[1], Kiran Kumar HB[3].

[1]Department of Biotechnology, the Oxford College of Engineering, Bengaluru, Karnataka, India

[2] Department of Biotechnology, NMAM Institute of Technology Affiliated to NITTE (Deemed to be University), Nitte, India

[3]Independent researcher, affiliated to Nrupathunga University, Bangalore, India

Corresponding Author: **Dr. BK Manjunatha**

Abstract: Hepatocellular carcinoma (HCC), a type of liver cancer is a major cause of morbidity and mortality (8.3%) globally. Increased knowledge of the molecular mechanisms underlying cancer progression has led to the development of large number of anticancer drugs. Several drawbacks of drug development such as tedious, time consuming, resource intensified process coupled with drugs failure in clinical trials and associated side-effects have necessitated plant based natural compounds as an alternative. Large body of scientific evidences now indicates that plant derived compounds or phytochemicals have significant antitumor properties. The results presented in this paper summarizes the data with respect to Scutellarein tetramethy lether (STE) a plant derived flavonoid and its anti-tumour activity in Hepatocellular adenocarcinoma cell line (HepG2).The cellular assays indicates cytotoxicity (MTT assay) of the compound at IC_{50} value of 47.49µM (16.2µg/ml), further it exhibited prominent Cell Cycle phase arrest at G2/M phase, S phase and Sub G0/G1 phasesandlate apoptosis. Finally, gene expression assay suggested it upregulated Caspase-3 gene and down regulated BCl2 gene. The molecular docking of STE against key HCC receptors revealed higher to moderate binding, with additional non-covalent interactions. The pharmacokinetic properties of the compound satisfy Lipinski drug likeness and good absorbability, solubility, and moderate crossing of the blood brain barrier. Finally, toxicity studies implicate lower hepatotoxicity and skin sensitization. In summary from the cellular and in silico analysis the natural compound STE could be considered as a lead candidate to perform future in-vitro and simulation studies towards development of a drug for the treatment of HCC.

Keywords: Notch, JAK/STAT, Stilbenoid, flavonoids and is of lavones, cyclin-dependent kinase (CDK)

1. Introduction

Hepatocellular carcinoma (HCC) is the most frequent cause of all liver cancers and constitutes 90% of cancers of liver globally. Approximately 7.5 Lakhs of new cases of HCC per year occurs globally which positions it as the 5th common cause of cancers (Shetty et.al., 2015; Ming Ren Toh et al., 2023; Satender P Singh et al., 2024). HCC is a complex multistep biological process that involves genetic and epigenetic alterations and environmental contribution (Ali Alqahtani et al., 2019). Malignant hepatocytes key cells affected in HCC are the result of changes accumulated in mature hepatocytes or derived from stem cells (Ágnes Holczbauer et al., 2022). Currently, the most accepted hypothesis describes sequential events which through external stimuli induce genetic alterations in mature hepatocytes leading to cell death, cellular proliferation, and the production of monoclonal Populations. (Elias Kouroumaliset al,2023). Several lines of research have shed light on the understanding of the critical oncogenic and tumor suppressor pathways involved in HCC. Signaling pathways, including TGF-β, Wnt/B-catenin, Notch, JAK/STAT, Hippo, and HIF are dis-regulated in HCC leading to uncontrolled cell division and metastasis (Zahra Farzaneh, et al., 2021). Targeting these cell signaling pathways provide an opportunity to identify novel targets (chemical/natural) that can be utilized for therapeutic development. Currently, the approved drug for advanced HCC is Sorafenib, which partially targets the multi-kinases involved in advanced liver cancer (Dimriet.al., 2020). Common side effects of Sorafenib affect multiple organs and physiological pathways include Fatigue, Nausea, Diarrhea, Abdominal pain, , Decreased appetite, Hair and Weight loss, Anemia, Hemorrhage blood pressure and Lymphopenia (cancer research uk). Phyto-constituents are non-nutrient active plant chemical compounds or bioactive compounds which improve treatment efficiency in cancer patients further, they have lower adverse reactions. The potential benefits of phytochemicals includes strengthening of immune system, reducing inflammation, preventing DNA damage and helping DNA repair, slowing cancer cell growth, regulating hormones and preventing damaged cells from reproducing. (Choundhari et.al., 2019).Several researchers have reported phytochemical exhibit multiple anticancer effects through several mechanism such as cytotoxicity, cell growth inhibition, cell cycle arrest, mitochondrial membrane potential disruption and apoptosis in HepG2 cells. Few examples include Resveratrol (Xiuyuan Ou et.al., 2014),Apigenin (Shou-Mei Wang et.al., 2021). Fucoxanthin (Langeswaran et.al., 2022), bioflavanone (Ratana Banjerdpongchai et.al., 2016). Stilbenoid, flavonoids and isoflavonesas natural sources of anti-tumour biomolecules have received attention from several researchers in the last 15 years. K S Huang and M Lin 1999 report anticancer activity of natural oligo stilbenesis modulated through multifaceted biological properties. Isorhapontigenin is a tetra hydroxylated stilbenoid with a methoxy group an isomer and analog of resveratrol found in several plants such as

Gnetumcleistostachyum, Aiphanes aculeata. Isorhapontin a glucoside is found in spruces, similarly Isorhapontigenin (ISOR) is found in Belamcanda chinensis. Its chemical structure is very similar to that of resveratrol and has antioxidative effect (Wang, (2001). It modulates oxidative stress-mediated signaling pathways, such as protein kinase C (PKC)-dependent phosphatidylinositol3-kinases (PI3K)-AKT-GSK3/p70S6K pathway(Yong Fang et.al., 2012).4',5,6,7-tetramethoxyflavone is a tetramethoxy flavone that is the tetra-O-methyl derivative of scutellarein has antimutagen properties. A plant metabolite derived as ascutellarein (Scutellarein 5, 6, 7, 4'-tetramethyl ether)(STE)belongs to the class of organic compounds known as 7-o-methylated flavonoid linked lipid molecule (Gianfranco Fontana et al., 2022). Within the cell, they are primarily located in the membrane, further biosynthesized from scutellarein. Outside of the human body, they are found asbioactive component of common sage and Siam weed extract. The compound exhibits anti-inflammatory activity through NF-κB pathway (Pandithet.al., 2013). Cyclooxygenase-2 (COX-2) and inducible nitric oxide synthase (iNOS) are critical pro-inflammatory proteins through which Scutellarein modulated anti-tumour activity (Eric W. C. Chan, et.al., 2019). Isowighteone is a member of the class of 7-hydroxyisoflavones that is isoflavone. These are polycyclic compounds containing a 2-isoflavene skeleton which bears a ketone group at the C4 carbon atom. A plant metabolite derived from isoflavone it is found in Ulexparviflorus, Ficusmucuso. Outside of the human body, isowighteone can be found in pigeon pea and pulses (Jun Wu et.al., 2024). By influencing key signaling pathways and metabolic processes, including the PI3K/AKT/mTOR, AMPK, and ROS pathways it modulates anti-cancer properties (Jibon Kumar Paul et al., 2024).

Molecular indicators of biological status, biomarkers, detectable in blood, urine, or tissue in HCC enable clinical management the disease states. Gold standard among these are the Apopain, or caspase 3, is a protease that executes apoptosis by cleaving various cellular proteins, Aurora-2 Aurora kinases play a crucial role in cell cycle regulation, particularly in mitosis(Aamir Ali and Todd Stukenberg 2023), C-Met growth factor binds to its receptor, c-Met, initiating a signalling cascade that can promote cell growth, migration, and survival (Yazhuo Zhang et al., 2018), EGFR (Epidermal growth factor receptor) activation leads to the activation of various downstream signalling pathways, including MAPK and STAT-3, which are involved in cell proliferation, survival, and metastasis(Ping Wee, Zhixiang Wang 2017), VEGFR a potent angiogenic factor that promotes the growth of new blood vessels(Zhen-Ling Liu et al., 2023), FGFR4 helps regulate bile acid synthesis in the liver, and its abnormal activation can contribute promotes tumor growth and PTEN acts as a tumor suppressor by regulating the PI3K/AKT pathway, which is crucial for cell growth and survival(Liwei Lang, Yong Teng et al., 2019). Current treatment

regime of HCC includes targeting these receptors through synthetic or natural compounds.

Discovery of new therapeutics is challenging, time-consuming and expensive enterprise. With the number of approved drugs declining steadily combined with increasing costs, a rational approach is needed to facilitate, expedite and streamline the drug discovery process. Towards this end computational methods are increasingly being implemented by several researchers and drug development chain largely assisted by developments in algorithms and greatly increased computer power (Thomas Leonard Joseph, 2017). Since, the tools can be applied at different stages: from target selection through identification of hits to optimization they have played key roles in several commercially available drugs and have become integral in the discovery of new drug discovery programs.

With this background the present study was carried out to investigate potential of bioactive compounds, Isorhapontigenin, Scutellarein tetramethyl ether and Isowighteone through molecular docking with HCC marker receptors and toxicity predictions. Also, in vitro assay of Scutellarein tetramethyl ether in HepG2 cell lines.

2. Methodology

All assays were carried out in a NABL laboratory under aseptic conditions. High quality analytical reagents were used and measures taken to exclude errors (Human, experimental errors).Standard protocols with few modifications were adhered to for all cellular assays.

a. Cellular assays

Cell lines and culture medium. The HepG2 (Human hepatocellular adenocarcinoma cell line) was procured from NCCS, Pune, India. The cells were maintained in DMEM low glucose media supplemented with 10 % FBS along with the 1% antibiotic-antimycotic solution in the atmosphere of 5% CO_2, 18-20% O_2 at 37^0C temperature in the CO_2 incubator and sub-cultured for every 2days.The cell was dissociated with the cell dissociating solution. The viability of the cells are checked and centrifuged. Further 20,000 cells/well was seeded in a 96 well plate and incubated for 24hrs at 37^0C, 5% CO_2 incubator.

MTT Assay. The cells were seeded (200µl cell suspension/20,000 cells/well) in a 96-well plate without the test agent about 24 hours. Appropriate concentrations of the test agent was added and incubated for 24hrs at 37°C in a 5% CO_2 atmosphere. After the incubation period spent media was removed, MTT reagent was added to a final concentration of 0.5mg/mL of total volume and incubated for 3 hours. The MTT reagent was removed and then 100µl of solubilization solution (DMSO) was added

the absorbance was read on a spectrophotometer or an ELISA reader at 570nm wavelength (Alley et.al., 1986).
% Cell viability is calculated using below formula % cell viability = [Mean abs of treated cells/Mean abs of Untreated cells] x 100.The IC_{50} value was determined by using linear regression equation i.e. Y =Mx+C. Here, Y = 50, M and C values were derived from the viability graph.

Cell cycle studies by flow cytometry. Cells were cultured at a density of 2 x 10^5 cells/2 ml in a 6-well plate and incubated in a CO_2 incubator overnight at 37°C for 24 hours. After aspiration the cells were treated with required concentration of experimental compounds and controls in 2 ml of culture medium and the cells were incubated for 24hours. The medium was removed from all the wells and washed with PBS and 500µl of trypsin-EDTA solution was added and incubated at 37°C for 5 minutes.2 ml culture medium was added and the cells were harvested directly into 12 x 75 mm polystyrene tubes and centrifuged for five minutes at 300 x g at 25°C. The supernatant was decanted carefully cells were fixed in 1ml of cold 70% ethanol and incubated for 30 minutes in -20˚C freezer. To ensure that only DNA is stained (PI stains all nucleic acids), cell pellet was treated with 400µL Propidium Iodide/RNase staining buffer and mixed well. Cells were then incubated for 15 to 20 minutes at room temperature in dark. Samples were analyzed by flow cytometry in PI/RNase solution (Kalejta et.al., 1997).

Apoptosis detection. Cells were cultured at a density of 0.5 x 10^6 cells/2 ml in a 6-well plate and incubated (CO_2) overnight at 37°C for 24 hours. After aspiration the cells were treated with required concentration of experimental compounds and controls in 2 ml of culture medium and the cells were incubated for 24 hours. The medium was removed and washed with PBS and 500µl of trypsin-EDTA solution was added and incubated at 37°C for 5 minutes.2 ml culture mediums was added and the cells were harvested directly into 12 x 75 mm polystyrene tubes and centrifuged for five minutes at 300 x g at 25°C. After decanting supernatant cells were washed twice with PBS and decanted completely. 5µl of FITC Annex in V was added, vortexed and incubated for 15 min at RT (25°C) in the dark. 5µl of PI and 400µl of 1X Binding Buffer was added and analyzed by flow cytometry (Homburg et.al., 1995).

Gene expression studies. Cells were cultured in a 6-well plate at a density of 0.5 x 10^6 cells/2 ml and incubated in a CO_2 incubator overnight at 37°C for 24 hours. The spent medium was aspirated and washed with 1ml 1X PBS and treated with required concentration of experimental compound and controls, in 1 ml of culture medium and incubated for 24 hours. One of the well was left as untreated and considered negative control. The mediumwas removed from all the wells into 12 x 75 mm

polystyrene tubes and washed with 500µl PBS (same tubes). The PBS was removed and 250µl of trypsin-EDTA solution was added and incubated at 37°C for 5 minutes and the cells were harvested directly into 12 x 75 mm polystyrene tubes. After centrifugation for 5 minutes at 300 x g at 25°C the supernatant was decanted carefully. Cells were then washed twice with PBS and decanted completely RNA was isolated by Qiagen RNeasy kit treated with DNAse and RNA quality and quantity by checked at 260/280 UV-Vis spectrophotometer and1.5% agarose gel respectively. cDNA synthesis was carried out using IScript cDNA synthesis kit (Cat No.1708890, Bio-Rad, CA).Reverse transcription reactions were assembled in an RNase-free environment and using standard protocol cDNA synthesis was carried out. The gene specific primers and a house keeping gene primer were validated by PCR using mixed pool of cDNA from given cells. Primers were then validated with SYBR reactions (Sensifast SYBR HiRoxkit, Bioline, USA) for amplification and melt curves. Gene expression study was carried out through relative quantification using Real Time PCR (Qiagen Rotor Gene Q 5plex HRM).ΔΔCt method was used for calculating fold changes. Fold changes >1 (housekeeping) was regarded as regulation (coded red) and < 1 is down regulation (coded green). (Porameesanaporn et.al., 2013).

B. In silico analysis

Retrieval of receptor and Ligand structure. The urls used in the study are listed in table-1.Receptor structures were downloaded from RCSB with their PDB ID's. 3D structures were downloaded in PDB www.rcsb.org format and 3D structures of selected ligands (Isorhapontigenin, Scutellarein tetramethyl ether and Isowighteone) were downloaded from pubchem in .sdf format (pubchem.ncbi.nlm.nih.gov). sdf format of ligands was converted to pdbqt format using Open Babel tool. Active site prediction was carried out using castP server. Grid box was created using values of x,y,z coordinates and saved in grid parameter file. Docking parameter was prepared by choosing Genetic Algorithm and each ligand was subjected to active site and file was saved and auto dock was performed.

Molecular visualization. The docking results visualization was carried out using Biovia Discovery Studio. The docked ligand and receptor were accessed in Discovery Studio. Ligand interaction was selected to view the 2D interaction between the ligand and receptor. The results of the docking (visualization) is displayed as amino acids residues that have roles in binding between the ligand and target protein.

Evaluation of drug likeliness of lead molecules and study of ADME Properties. Structure of Isorhapontigenin, Scutellareintetramethyl ether and Isowighteone were downloaded from pubchem in .sdf format. The files were converted from .sdf format to pdb format using Open Babel and the pdb format was input to SCFbio online

server to validate Lipinski rule of five. Toxicity prediction of the chosen ligands Isorhapontigenin, Scutellarein tetramethyl ether and Isowighteone was carried out using pkCSM online tool by entering the SMILES format of the compounds.

3. Results

a. Cellular assays

MTT Assay

The percentage cell viability and concentration of test drug needed to inhibit cell growth by 50% (IC_{50}) was generated from the cell viability graph.IC_{50} value of 47.49µM (16.2µg/ml) was derived from a linear regression analysis. The data is summarized in table-2, figure-2,3.

Cell cycle studies

In Sub G0/G1 phase (Apoptotic phase), 0.39%, 20% and 15.22% of cells were arrested in Untreated, Standard and STE with IC_{50} concentration respectively. In G0/G1 phase (Growth Phase), 57.31%, 46.58% and 14.26% of cells were arrested. In S phase (synthetic phase), 9.4%, 9.47% and 16.91% of cells were arrested respectively. Finally, in G2/M phase (Metaphase), 30.03%, 20.16%, and 40.8% of cells were arrested (Table-3, Figure-4,5).

Apoptosis detection

The table-4 summarizes the % of cells which have undergone apoptosis and necrosis in after untreated, standard control and Doxorubicin treatment with 3uM/ml and STE and 47.49µM concentration treated HepG2 cells in comparison to viable cells. Cells treated with 3µM of Doxorubicin had undergone necrosis and late apoptosis in HepG2 cells with 14.8% and 65.97% respectively. Whereas, in Scutellarein tetramethyl ether (STE) treatment 44.79% of cells had undergone late apoptosis (Figure-6). Figure 7is a schematic quadrangular plot (Annexin V/PI expression) representation of cells in apoptosis the test compound-STE at 47.49µM concentration and Doxorubicin at 3uM concentration. Analysis was done by using BD FACS calibur, Cell Quest Pro Software (Version: 6.0). Here, Annexin V- FITC was used as Primary Marker, and PI- Propidium as Iodide Secondary fluorescence Marker.

Gene expression studies.RNA gel to quantity the RNA is illustrated in figure-8. Effect of Scutellarein tetramethyl ether on Caspase-3 and Bcl2 gene expression were studied in HepG2 cells by Real time quantitative PCR with Beta-Actin as the internal control. To determine the gene expression values, raw fluorescence data (Ct values) generated were exported to Rotor-Gene Q software version 2.3.4 and using the formula for relative quantities: ΔCt = Average Ct of test sample - Average Ct of calibrator

The ΔCt values will be converted to a linear form using the formula: E-ΔCt, Where E=amplification efficiency.
To calculate the expression of a target gene (TG) relative to the EC, the comparative Ct (ΔΔCt) method 148 (Step one Software v2.2.2) was used as per the following equation: ΔΔCt = (Ct Target gene)-(Ct EC) – (Ct Target gene)-(Ct EC).Test Sample Calibrator.
The ΔΔCt values are converted to a linear form using the formula: E –ΔΔCt. Relative expression is a variation of the expression of a gene between two samples. The RQ (Relative quantification value) is the fold change compared to the calibrator (untreated sample, time zero, etc.). The BCL2 gene expression was downregulated by 0.333folds (50% lower) when compared to the standard control which has a fold change of 0.666.The gene expression of caspase-3gene was upregulated by 4.303 folds which is close to the standard fold change value(Figure-9). The fold expression was calculated with the observed Ct values for each gene with respect to the treated and untreated samples. The obtained results suggest that relative gene expression level of Caspase-3 gene was up regulated and BCl2 gene was down regulated in treated groups compared to untreated group (Figure-10).

b. In silico analysis

Evaluation of drug likeliness of lead molecules
Lipinski rule with the following criterion were used in the analysis

- Molecular mass less than 500 Dalton
- High lipophilicity (expressed as LogP less than 5)
- Less than 5 hydrogen bond donors
- Less than 10 hydrogen bond acceptors
- Molar refractivity should be between 40-130

These filters help in early preclinical development and could help avoid costly late-stage preclinical and clinical failures. The data is summarized in tables-5.
Docking studies. Molecular docking was done using Autodock along with MGL tools. The results were visualized using Biovia Discovery Studio. The results revealed that Isorhapontigenin, Isowighteone and Scutellarein tetramethyl ether formed different hydrophobic interactions with the selected receptors.

Docking studies of Isorhapontigenin

a. Isorhapontigenin was docked to Apopain, Aurora-2, C-MET, EGFR, FGFR4, PTEN and VEGFR-2. Various hydrophobic interactions like vander waal's interaction, pi-alkyl bonds, conventional hydrogen bonds and carbon hydrogen bonds were observed. Table 6, summarizes the binding energy values and hydrogen bonds

formed between Isorhapontigenin and receptors. Figures-11(a-g) represents the 3D and 2D interaction between Isorhapontigenin with various receptors-Apopain (1CP3), Isorhapontigenin and C-MET(2RFN), Isorhapontigenin and EGFR, Isorhapontigenin and FGFR4(4XCU), Isorhapontigenin and PTEN(1D5R), Isorhapontigenin and VEGFR (4MXC),respectively.Table-6-Summary of Various bonds formed between Isowighteone and receptors.Table-7 summarizes the binding energy values and hydrogen bonds formed between Isorhapontigenin and receptors.

b. Isowighteone was docked to Apopain, Aurora-2, C-MET, EGFR, FGFR4, PTEN and VEGFR-2. Various hydrophobic interactions like vanderwaal's interaction, alkyl bonds, pi-alkyl bonds, conventional hydrogen bonds and carbon hydrogen bonds were observed. Figures-12(a-g) represents the 3D and 2D interaction between Isowighteone with various receptors-Apopain (1CP3), Isowighteone and Aurora-2(2BMC), Isowighteone and C-MET(2RFN), Isowighteone and EGFR(5D41), Isowighteone and FGFR4(4XCU), Isowighteone and PTEN(1D5R), Isowighteone and VEGFR(4MXC). Table-8summarizes the binding energy values and hydrogen bonds formed between Isorhapontigenin and receptors. Table-9summarizesbinding energy values and hydrogen bonds formed between Isowighteone and receptors.

c. Based on the in vitro studies, Scutellarein tetramethyl ether was docked to Apopain, Aurora-2, C-MET, EGFR, FGFR4, PTEN and VEGFR-2 and Cox2, TNF-alpha TERT, AKT1, PDGFR and BCL2.Figures-13(a-p)represent the 3D and 2D interaction between Scutellarein tetramethyl ether and Apopain(1CP3), Scutellarein tetramethyl ether and Aurora-2(2BMC), Scutellarein tetramethyl ether and C-MET(2RFN), Scutellarein tetramethyl ether and EGFR(5D41), Scutellarein tetramethyl ether and FGFR4(4XCU), Scutellarein tetramethyl ether and PTEN(1D5R), Scutellarein tetramethyl ether and VEGFR(4MXC) , Scutellarein tetramethyl ether and NFkB(1SVC), Scutellarein tetramethyl ether and Cox2(4FM5), Scutellarein tetramethyl ether and TNF-alpha(6OOY), Scutellarein tetramethyl ether and TNF(2TNF), Scutellarein tetramethyl ether and PI3K(4FJZ), Scutellarein tetramethyl ether and TERT (3DU6), Scutellarein tetramethyl ether and AKT1(3CQU), Scutellarein tetramethyl ether and PDGFR∝ (5K5X), Scutellarein tetramethyl ether and VEGFR2(2OH4), Scutellarein tetramethyl ether and BCL2 (2W3L) respectively. Table 10 summarizes the binding energy values and hydrogen bonds formed between Scutellarein tetramethyl ether and receptors. Table-11.Summary of various bonds formed between Scutellarein tetramethyl ether and receptors.

Pharmacokinetic (ADME) properties are summarized in table-12. Of the three compounds STE displayed range of spectrum of properties. Absorption (-4.426),

intestinal absorbption and P-glycoprotein I inhibition, distribution (VDss-human --0.112) and blood brain barrier (BBB) permeability (-0.586), metabolism (through CYP450), excretion total clearance and max. tolerated dose in human (0.153Log/mg/kg/day)and finally toxicity-Oral Rat Chronic Toxicity (2.4-mol/kg) and no Hepatic or skin toxicity.

4. Discussion

Cancer, an ever-increasing global disease is not a single process, multitude of mechanisms including initiation; promotion and progression contribute to the final pathology. Hepatocellular carcinoma constitutes more than 90% of the primary tumor of the liver. Cirrhosis is a significant step in viral carcinogenesis for hepatocellular carcinoma. Malignant tumor hepatocytes are distinguished by cytological features trabecular architectural pattern, pseudoacinar (acinar with proteinaceous material), compact and sarcomatoid (Hepatocellular Carcinoma – Stat Pearls 2023).Multiple lines of research indicate that plant derived compounds or phytochemicals have significant antitumor properties (Sheryl Rodriguez et al., 2021). In the present study Stilbenoid, flavonoids and isoflavones natural sources of anti-tumour biomolecules were assessed for their anti- Hepatocellular Carcinoma potential using cellular assays and in silico studies. The potential of STE as a HCC anti-tumor compound was assessed by in vitro assays on HepG2 (Hepatocellular adenocarcinoma cell line). The results of cytotoxicity study performed by MTT assay suggest that the test compound, STE is cytotoxic in nature at an IC_{50} value of 47.49µM (16.2µg/ml). STE exhibited prominent Cell Cycle phase arrest at G2/M phase, S phase and Sub G0/G1 phase on HepG2 cells. The results implicate the compound has potential to disrupt the cell cycle and prevent cancer cell proliferation. The results supplement the finding of previous study of corroborating the cell-cycle arrest function of flavonoids. Previous studies have shown flavonoids interact with regulators cyclin-dependent kinase (CDK) 4/6-cyclin D and CDK1-cyclin B complexes to arrest cell-cycle, hence from the afore observations and previous research evidences we could infer that the STE could also have similar role (Saha, A et al., 2020).

STE treatment induced apoptosis in 44.79% of cells compared to Doxorubicin where 14.8% and 65.97% cells had undergone necrosis and late apoptosis in respectively. Apoptosis, or programmed cell death, is a promising target in cancer treatment since cancer cells often evade apoptosis, leading to uncontrolled growth and resistance to therapies (Benedito A Carneiro and Wafik S El-Deiry 2020). The advantage of STE as a natural compound and its apoptosis inducing properties underscores its potential in HCC treatment. Gene expression suggested that the level of Caspase-3 gene was up regulated and BCl2 gene was down regulated in treated group when compared to untreated group. Caspase3 (cysteine aspartases,

or cysteine-dependent aspartate-directed proteases) belong to the family of proteases with roles in regulation of apoptosis and inflammatory processes. During the intrinsic activation, to process the Caspase-3 zymogen, the mitochondrial cytochrome c collaborates with apoptosis-activating factor 1 (Apaf-1), ATP, and Caspase-9. Proteins of the Bcl-2 family, including pro- and anti-apoptotic members of the family, regulate mitochondrial outer membrane permeability, which plays an important role in the control of apoptosis. pro-apoptotic proteins of the Bcl-2 family may induce, and anti-apoptotic members may inhibit, cytochrome c liberation into the cytosol; after which, the activation of Caspase-3 and Caspase-9 leads to apoptosis. (Piret Hussar 2022). Extrapolating the results from gene expression studies to the apoptosis data it could be proposed that STE induces apoptosis through the BCL2/ Caspase pathway.

In silico methods have been playing an important role in rational drug design, thereby aiding the speed and the rate of production and screening of drug candidates (Yiqun Chang 2022). Facilitating analysis of calculated properties, prediction models for drug therapeutic targets and identification of safety liabilities in silico methods minimize the need for time and the attrition rate of failures in drug development. Molecular docking was carried out with compounds Isorhapontigenin, Isowighteone and STE against HCC receptors. Isorhapontigenin binding energy was higher with EGFR (-11.33/Kcal/mol), whereas Isowighteone bound to Apopain (-11.83), EGFR (-13.81) VEGF (-13.03), and Kcal/ molenergies. Finally binding energy of STE to Apopain, VEGFR and EGFR was -10.57,-12.37 and -11.51(Kcal/mol) respectively. The results also revealed that STEapart from conventional hydrogen, covalent hydrogen bond and vanderwaals bonds, other bonds Pi-sigma Pi-Cation Alkyl, Pi-Alkyl were also observed. Thenon-covalent interactions along with hydrogen bonds and van der Waals forces contribute to the overall binding stability and specificity and are crucial for the affinity of a ligand to a protein. Predicting and analyzing these types of interactions, aid in drug design and development (Rajagopalan Vaidyanathan et al., 2023). In comparison to Isorhapontigenin and Isowighteone the Lipinski physicochemical parameters and its values of STE was higher with Mass of 342, and Molar refractivity of 83.87.The data is suggestive of its better bioavailability and absorption. With respect to the spectrum of pharmacokinetic properties, STE showed water solubility distribution and excretion. The compound was selectively metabolized through Cytochrome P450 (CYP450 enzymes), these enzymes are responsible for the metabolism of several synthetic and natural medications. Finally the compound demonstrated low hepatic and skin toxicity. Previous studies have implicated the drug has better bioavailability and kinetic properties (Nguyen ThiThoa, Ninh the Son et al., 2025).

Cumulatively, the cellular assays and docking studies suggest STE has potent HCC activity modulated through cell-cycle and bcl-2 mediated apoptosis. Further, the results of docking demonstrated the compound binds to several HCC receptors and forms range of covalent and non-covalent interactions suggesting a stronger ligand-receptor interaction. Finally the bioavailability and toxicity further augment it as a lead candidate natural compound to perform future in-vitro, in-vivo and pharmacological studies.

References

1. VijithVittal Shetty, AdithiKellarai. Comprehensive Review of Hepatocellular Carcinoma in India: Current Challenges and Future Directions. JCO Glob Oncol. 2022 Oct: 8: e2200118.
2. Ming Ren Toh, Evelyn Yi Ting Wong, Sunny Hei Wong, Alvin Wei Tian Ng, Lit-Hsin Loo, Pierce Kah-Hoe Chow, Joanne Ngeow Global Epidemiology and Genetics of Hepatocellular Carcinoma. Gastroenterology. 2023 Apr; 164(5): 766-782.
3. Satender P Singh, Tushar Madke, Phool Chand. Global Epidemiology of Hepatocellular Carcinoma J Clin Exp Hepatol. 2025 Mar-Apr; 15(2):102446.
4. Ali Alqahtani, Zubair Khan, Abdurahman Alloghbi, Tamer S Said Ahmed, Mushtaq Ashraf, Danae M Hammouda. Hepatocellular Carcinoma: Molecular Mechanisms and Targeted Therapies.Medicina (Kaunas). 2019 Aug 23; 55(9):526.
5. Ágnes Holczbauer, Kirk J. Wangensteen, Soona Shin. Cellular origins of regenerating liver and hepatocellular carcinoma. JHEP Reports Volume 4, Issue 4, April 2022, 100416.
6. Elias Kouroumalis, Ioannis Tsomidis, Argyro Voumvouraki. Pathogenesis of Hepatocellular Carcinoma: The Interplay of Apoptosis and Autophagy. Biomedicines 2023, 11(4), 1166.
7. Zahra Farzaneh, Massoud Vosough, Tarun Agarwal, Maryam Farzaneh. Critical signaling pathways governing hepatocellular carcinoma behavior; small molecule-based approaches Cancer Cell Int. 2021 Apr 13; 21:208.
8. Manali Dimri, Ande Satyanarayana. Molecular Signaling Pathways and Therapeutic Targets in Hepatocellular Carcinoma. Cancers (Basel). 2020 Feb 20;12(2):491. www.cancerresearchuk.org.
9. Amit S Choudhari, Pallavi C Mandave, Manasi Deshpande, Prabhakar Ranjekar, Om Prakash. Phytochemicals in Cancer Treatment: From Preclinical Studies to Clinical Practice. Front Pharmacol. 2020 Jan 28; 10:1614.

10. Xiuyuan Ou, Yan Chen, Xinxin Cheng, Xumeng Zhang, Qiyang He. Potentiation of resveratrol-induced apoptosis by matrine in human hepatoma HepG2 cells. Oncol Rep. 2014 Dec; 32(6): 2803-9.
11. Expression of micro RNA Transcriptome. Front Oncol. 2021 Apr 6:11:657665.
12. Sangavi, K Langeswaran, S Gowtham Kumar Anticarcinogenic Efficacy of Fucoxanthin on HepG2 Cell LinesXC05-XC09.Journal of Clinical and Diagnostic Research. 2022. Volume : 16. Issue : 2. Page : XC05 - XC09.
13. Ratana Banjerd pongchai, Benjawan Wudtiwai, Patompong Khaw-on, Wasitta Rachakhom, Natthachai Duangnil, Prachya Kongtawelert, Hesperidin from Citrus seed induces human hepatocellular carcinoma HepG2 cell apoptosis via both mitochondrial and death receptor pathways. Tumour Biol. 2015 Jul 21; 37(1):227–237.
14. K S Huang, M Lin. Oligostilbenes from the roots of Vitis amurensis. J Asian Nat Prod Res. 1999; 2(1):21-8.
15. Q L Wang, M Lin, G T Liu. Antioxidative activity of natural isorhapontigenin. Jpn J Pharmacol. 2001 Sep; 87(1):61-6.
16. Yong Fang, Yonghui Yu, Qi Hou, Xiao Zheng, Min Zhang, Dongyun Zhang, Jingxia Li, Xue-Ru Wu, Chuanshu Huang. The Chinese herb isolate isorhapontigenin induces apoptosis in human cancer cells by down-regulating overexpression of antiapoptotic protein XIAP. J Biol Chem. 2012 Oct 12; 287(42): 35234-35243.
17. Gianfranco Fontana, Maurizio Bruno, Francesco Sottile, Natale Badalamenti. The Chemistry and the Anti-Inflammatory Activity of Polymethoxy flavonoids from Citrus Genus. Antioxidants (Basel). 2022 Dec 22; 12(1):23.
18. Hataichanok Pandith, Xiaobo Zhang, Suchitra Thongpraditchote, Yuvadee Wongkrajang, Wandee Gritsanapan, Seung Joon Baek. Effect of Siam weed extract and its bioactive component scutellarein tetramethyl ether on anti-inflammatory activity through NF-κ Bpathway. J Ethnopharmacol. 2013 May 20; 147(2): 434-41.
19. Eric W. C. Chan, Carine S. S. Lim, Win Yee Lim, ZhiJuin Loong, Chen Wai Wong. Role of scutellarin in human cancer, A review. J Appl Pharm Sci, 2019; 9(01): 142. 146.
20. Jun Wu, Qian Zhou, Chenhaojin Zhou, Ka-Wing Cheng, Mingfu Wang Food frontiers. Strategies to promote the dietary use of pigeon pea (Cajanuscajan L.) for human nutrition and health. Jun Wu, Qian Zhou, Chenhaojin 2024. Volume 5. issue3.
21. Jibon Kumar Paul, Mahir Azmal, ANM Shah Newaz Been Haque, Omar Faruk Talukder, Meghla Meem, Ajit Ghosh. Phytochemical-mediated modulation of signaling pathways: A promising avenue for drug discovery. Advances in Redox Research Volume 13, December 2024, 100113.

22. Aamir Ali, Todd Stukenberg. Aurora kinases: Generators of spatial control during mitosis.Front. Cell Dev. Biol., 13 March 2023.Sec. Cell Growth and Division. Volume 11 - 2023.
23. Yazhuo Zhang, Mengfang Xia, KeJin, Shufei Wang, Hang Wei, Chunmei Fan, Yingfen Wu, Xiaoling Li, Xiayu Li, Guiyuan Li, Zhaoyang Zeng & Wei Xiong. Function of the c-Met receptor tyrosine kinase in carcinogenesis and associated therapeutic opportunities. Molecular Cancer volume 17, Article number: 45 (2018).
24. Ping Wee, Zhixiang Wang. Epidermal Growth Factor Receptor Cell Proliferation Signaling Pathways. Cancers (Basel). 2017 May 17; 9(5): 52.
25. Zhen-Ling Liu, Huan-Huan Chen, Li-Li Zheng, Li-Ping Sun & Lei Shi. Angiogenic signaling pathways and anti-angiogenic therapy for cancer. Signal Transduction and Targeted Therapy volume 8, Article number: 198 (2023).
26. Liwei Lang, Yong Teng. Fibroblast Growth Factor Receptor 4 Targeting in Cancer: New Insights into Mechanisms and Therapeutic Strategies. Cells. 2019 Jan 9; 8(1):31.
27. Leonard, Joseph, Namasivayam, Vigneshwaran, Poongavanam, Vasanthanathan, Kannan, Srinivasaraghavan. In Silico Approaches for Drug Discovery and Development. (2017). 3-74 (72).
28. Michael C. Alley; Dominic A. Scudiero; Anne Monks; Miriam L. Hursey; Maciej J. Czerwinski; Donald L. Fine; Betty J. Abbott; Joseph G. Mayo; Robert H. Shoemaker; Michael R. Boyd. Feasibility of Drug Screening with Panels of Human Tumor Cell Lines Using a Microculture Tetrazolium Assay. Cancer Res (1988) 48 (3): 589–601.
29. R F Kalejta, T Shenk, A J Beavis. Use of a membrane-localized green fluorescent protein allows simultaneous identification of transfected cells and cell cycle analysis by flow cytometry.Cytometry.1997 Dec 1; 29 (4):286-91.
30. Christa H.E. Homburg, Masja de Haas, Albert E.G.Kr. vondem Borne, Arthur J. Verhoeven, Chris P.M. Reutelingsperger, Dirk Roos. Human Neutrophils Lose Their Surface FcγRIII and Acquire Annexin V Binding Sites During Apoptosis In Vitro. Blood. Volume 85, Issue 2, 15 January 1995, Pages 532-540.
31. Y. Porameesanaporn, W. Uthaisang-Tanechpongtamb, F. Jarintanan, S. Jongrungruangchok, B.T. Wongsatayanon. Terrein induces apoptosis in HeLa human cervical carcinoma cells through p53 and ERK regulation. Oncol. Rep., 29 (2013), pp. 1600-1608.
32. www.rcsb.org.
33. pubchem.ncbi.nlm.nih.gov.
34. www.ncbi.nlm.nih.gov.

35. Sheryl Rodriguez, Kristy Skeet, Tugba Mehmetoglu-Gurbuz, Madeline Goldfarb, Shri Karri, Jackelyn Rocha, Mark Shahinian, Abdallah Yazadi, Seeta Poudel, Ramadevi Subramani. Phytochemicals as an Alternative or Integrative Option, in Conjunction with Conventional Treatments for Hepatocellular Carcinoma. Cancers (Basel). 2021 Nov 17; 13(22): 5753.
36. Saha, A., Ghosh, D and Das, P. (2020). Anticancer properties of natural compounds: Insights into molecular mechanisms and therapeutic potential. Phytochemistry Reviews, 19(4), 679-703.
37. Benedito A Carneiro, Wafik S El-Deiry. Targeting apoptosis in cancer therapy.Nat Rev ClinOncol. 2020 Jul;17(7):395-417.
38. PiretHussaria.Apoptosis Regulators Bcl-2 and Caspase-3.Encyclopedia 2022, 2(4), 1624-1636.
39. Yiqun Chang, Bryson A Hawkins, Jonathan J Du, Paul W Groundwater, David E Hibbs, Felcia Lai. A Guide to In Silico Drug Design. Pharmaceutics. 2022 Dec 23; 15 (1):49.
40. Rajagopalan Vaidyanathan, Sangeetha Murugan Sreedevi, Keerthiga Ravichandran, Seba Merin Vinod, Yogesh Hari Krishnan, Lalith Kumar Babu, Parimala Selvan Parthiban, Lavanya Basker, Tamizhdurai Perumal, Vasanthi Rajaraman, Gopala krishnan Arumugam, Kumaran Rajendran, Vanjinathan Mahalingam. Molecular docking approach on the binding stability of derivatives of phenolic acids (DPAs) with Human Serum Albumin (HSA): Hydrogen-bonding versus hydrophobic interactions or combined influences? JCIS Open Volume 12, December 2023, 100096.
41. Nguyen Thi Thoa, Ninh the Son. Scutellarein: a review of chemistry and pharmacology. Journal of Pharmacy and Pharmacology, Volume 77, Issue 3, March 2025, Pages 352–370.

Tables and figures

Table 1.url resources used in the present study

Data base	Purpose	Web links
PDB	Retrieval of receptors	www.rcsb.org
Pubchem	Retrieval of Compounds	pubchem.ncbi.nlm.nih.gov
Open babel	Convert and analyse structure formats	openbabel.org
Auto dock and MGL tools	Docking	mgltools.scripps.edu

Cast P	To find possible binding pockets and their surface area	sts.bioe.uic.edu
Pk CSM	Toxicity prediction	biosig.unimelb.edu.au
SCF bio	To determine drug likeliness	www.scfbio-iitd.res.in

Table 2. Cell viability and IC_{50} values for the standard and the test compounds

Concentration unit: µM/ml		**Incubation: 24hrs**		**Cell line: HepG2**				
Parameter	Blank	Untreatd	Std control	6.25	12.5	25	50	100
Abs reading 1	0.042	0.864	0.379	0.802	0.713	0.582	0.425	0.107
Abs reading 2	0.051	0.881	0.392	0.785	0.728	0.595	0.41	0.084
Mean abs	0.046	0.872	0.385	0.793	0.720	0.588	0.417	0.095
Mean abs(Sample-blank)		0.826	0.339	0.747	0.647	0.542	0.371	0.049
Standard deviation		0.012±0.08	0.009±0.006	0.012 ±0.008	0.0106 ±0.007	0.009 ±0.006	0.010 6±0.007	0.016 ±0.011
Cell Viability		100	41.04	90.43	81.59	65.61	44.91	5.93

Table 3. HepG2 cells (%) arrested in different phases of cell cycle

% cells arrested in different cell cycle phases of HepG2				
Sl No	**Cell Cycle stage**	**Untreated**	**Std control**	**STE**
1	Sub G0/G1	0.39	20	15.22
2	G0/G1	57.31	46.58	14.26
3	S	9.4	9.47	16.91
4	G2/M	30.03	20.16	40.8
Total events selected per each group -10000				

Table 4. Hep G2 cells (%) under gone apoptosis in untreated, standard and test compounds

	%Necrotic cells	%Late apoptotic cells	%Viable cells	%Early apoptotic cells
Label	UL	UR	LL	LR
Untreated	4.64	6.13	89.15	0.08
Std control	14.8	65.97	18.99	0.24
STE	11.28	44.79	32.46	11.47

Table 5. Lipinski parameter and its values for the compounds

a. Isorhapontigenin:

Parameter	Value
Mass	258
Hydrogen bond donor	3
Hydrogen bond acceptors	4
LOGP	1.58
Molar refractivity	64.88

b. Isowighteone:

Parameter	Value
Mass	338
Hydrogen bond donor	3
Hydrogen bond acceptors	5
LOGP	2.45
Molar refractivity	87.61

c. Scutellarein tetramethyl ether

Parameter	Value
Mass	342
Hydrogen bond donor	0
Hydrogen bond acceptors	6
LOGP	3.03
Molar refractivity	83.87

Table 6.Binding energy values and hydrogen bonds formed between Iso wighte one and receptors

Receptor	Pdb id	Binding affinity (Kcal/mol)	No of hydrogen bonds formed
Apopain	1CP3	-9.27	2
Aurora-2	2BMC	-8.08	3
C-Met	2RFN	-4.05	2
EGFR	5D41	**-11.33**	2
FGFR4	4XCU	-10.01	0
PTEN	1D5R	-10.52	4
VEGFR	4MXC	-9.87	2

Table 7. Summary of Various bonds formed between Isorhapontigenin and receptors

Receptor/ Binding energy kcal/mol	**Conventional hydrogen bonds(Amino acid residues)**	**Covalent bonds(Amino acid residues)**	**vanderwaal's interaction (Amino acid residues)**	**Non-covalent bonds**	**Pi-Donor Hydrogen bond**
Aurora-2(2BMC) -8.08	SER A:314, TRP A:313 and ASP A:307	LYS A: 309 and ASP A: 311.	ARG A: 255, ASP A: 256, GLU A:308, HIS A:206, ASP A:311, LYS A:309, ARG A:371 and LEU A:312.		

C-MET(2RFN) -4.05	ALA A:1189 and SER A:1197	MET A:1192 and TYR A:1194.		VAL A:1334.	
EGFR(5D41) -11.33	ARG A:705 and LEU A:707	CYS B:781 and GLY A:779.	ILE B:789, ILE B:706, LEU B:760, LEU B:759, LEU B:788, CYS B:781, ILE B:759, VAL B:786 and GLN B:787.	LEU B:782, LEU B:789 and ALA A:763.	
FGFR4(4XCU) -10.01	TYR A:643 and LYS A:645.	PRO A:652.	TYR A:643, TYR A:642, LEU A:651, LYS A:645 and THR A:646.	ASP A:641	
PTEN(1D5R) -10.52	ASP A:115, SER A:113, ASP A:107 and GLU A:106	TRP A:111 and ASP A:109.	LEU A: 112, TRP A:111, ASP A:109 and LEU A:108.		
VEGFR(4MXC) 9.87	GLY A:1085 and SER A:1111	GLY A:1090 and VAL A:1092.	VAL A: 10833, VAL A:1092, LYS A:1110, VAL A:1109, GLY A:1087, ASN A:1113 and GLY A:1090.	ARG:1086.	TYR A:1093

Table 8. Binding energy values and hydrogen bonds formed between Isowighteone and receptors.

Receptor	Pdb id	Binding affinity(kcal/mol)	No of hydrogen bonds formed
Apopain	1CP3	**-11.83**	2
Aurora-2	2BMC	-9.47	1
C-Met	2RFN	-10.87	3
EGFR	5D41	**-13.81**	1
FGFR4	4XCU	-10.39	2
PTEN	1D5R	-11.79	1
VEGFR	**4MXC**	**-13.03**	1

Table- 9.Summary of Various bonds formed between Isorhapontigenin and receptors

Receptor/ Binding energy kcal/mol	Conventional hydrogen bonds(Amino acid residues)	Covalent bonds(Amino acid residues)	Vander waal's interaction (Amino acid residues)	Non-covalent bonds	Pi-Donor Hydrogen bond
Apopain(1CP3) -11.83	THR A:92 and MET A:100	VAL A:97 and GLU A:95.	ASN A:52, GLY A:129, ILE A:127, ILE A:139, ARG A:93, GLU A:94, GLU A:95, VAL A:97, GLU A:98 and LEU A:99.	VAL A:134, ILE A:50 and LEU A:91	
Aurora-2(2BMC) -9.47	VAL A:206.	PHE A:165 and VAL A:163.	LEU A:169, LYS A:162 and LEU A:208.	LYS A:166, PHE A:144, ARG A:205, GLY A:145, VAL A:163, TYR A:207 and LEU A:178.	
C-MET(2RFN) -10.87kcal/mol	ALA A:1189, LEU A:1181 and ILE A:1182	LEU A:1186 and PHE A:1184.	PHE A:1269, ILE A:1337, GLN A:1187, LEU A:1186, PHE A :1184, GLY A:1183, LEU A:1276, LEU A:1273 and VAL A:1188.		
EGFR(5D41) -13.81	TYR B:727	ALA B:743 and LYS B:745.	LYS B:745, LYS B:713, GLY B:729, VAL B:742,		ILE B:789 and LYS B:714.

			ALA B:743, THR B:725, PHE B:712, LEU B:788 and THR B:725.		
FGFR4(4XCU) -10.39	CYS A:725 and GLU A:717	GLY A:720 and MET A:722.	ARG A:723, GLY A:720, TYR A:719, MET A:722, GLU A:724, LEU A:739, LEU A:743, LEU A:718 and VAL A:746.		ALA A:742.
PTEN(1D5R) -11.79	LEU A:193	PRO A:248 and CYS A:250.	PHE A:195, PHE A:347, LEU A:247, PRO A:248, LEU A:194, VAL A:191, ALA A:192, CYS A:250, GLN A:219 and THR A:277.		ILE A:253.
VEGFR(4MXC) 13.03	LEU A:1154	LEU A:1147 and ILE A:1145.	LEU A:1147, ILE A:1145, PRO A:1153, VAL A:1155 and VAL A:1156.		ILE A:1076, ILE A:1071, ARG A:1148 and PRO A:1073.

Table-10: Binding energy values and hydrogen bonds formed between Scutellarei tetramethyl ether and receptors

Receptor	Pdb id	Binding affinity(kcal/mol)	No of hydrogen bonds formed
Apopain	1CP3	-10.57	3
Aurora-2	2BMC	-9.18	2
C-Met	2RFN	-5.40	0
EGFR	**5D41**	**-11.51**	0
FGFR4	4XCU	-9.88	3
PTEN	1D5R	-10.81	4
VEGFR	4MXC	**-12.37**	1
NF-kB	1SVC	-7.73	0
Cox-2	4FM5	-9.96	0
TNF-∝	6OOY	-8.96	1
TNF	2TNF	-9.21	2
PI3K	4FJZ	-8.84	1
TERT	3DU6	-9.11	1
AKT1	3CQU	-9.37	1
PDGFR∝	5K5X	-9.95	0
VEGFR2	2OH4	-8.04	1
BCL2	2W3L	-8.83	0

Table 11. Summary of various bonds formed between Scutellarein tetramethyl ether and receptors

Receptor/ Binding energy kcal/mol	Conventional hydrogen bonds(Amino acid residues)	Covalent bonds(Amino acid residues)	vanderwaal's interaction (Amino acid residues)	Non-covalent bonds	Pi-Donor Hydrogen bond	Pi-sigma
Apopain(1CP3) 11.83	PHE A: 247, ALA A: 244 and ASP A: 169	LYS A: 259 and GLN A: 261.	THR A: 245, TRP A: 214, GLN A: 261, GLY A: 171, LYS A: 259, TRP A: 206 and CYS A: 170.	GLU A: 248.		

Aurora-2(2BMC) 9.18kcal	PHE A:144 and GLY A:145.				LYS A:162,	LEU A:178.
C-MET(2RFN) 5.40	A:1220 and ASP A:1222.		LEU A:1140, ALA A:1221 and GLY A:1128.			MET A:1131.
FGFR4(4XCU) 9.88	A:647,ARG A:559 and ARG A:616	ASP A:641.	ASN A:648. ASN A:557,ASN A:617 and LYS A:645.			THR A:646
PTEN(1D5R) 10.81	LYS A:125,ARG A:130,CYS A:124 and HIS A:93.	GLN A:171.	THR A:131and GLY A:129.		ASP A:92.	VAL A:45
VEGFR(4MXC) 12.37	GLY A:1163	LYS A:1161 and TYR A 1159.		LEU A:1140, LYS A:1219 and MET A:1211.		
NFkB(1SVC) -7.73	LYS P:148, THR P:205, MET P:208 and LYS P:206.	PHE P:151, LYS P:149, GLU P:152 and LEU P:210.		VAL P:150 LYS P:147.		
Cox2(4FM5) 7.73	ASN A:38, GLU A:465, SER A:471, ARG A:469,ASN A:42 and LYS A:468.		CYS A:40,GLN A:41 and LEU A:472.	ARG A:43		
TNF-alpha(6OOY) 9.96	PHE A:144	LEU A:142, ASP A:143 and GLU	LYS A:65, ASP A:140, GLY A:24	ALA A:145.		

		A:23.	and PRO A:139.			
TNF(2TNF) 9.21	CYS A:69 and LYS A:112.		TRP A:114, THR A:105 and CYS A:101.			PRO A:106.
PI3K(4FJZ) 8.84	ASP A:964.		ALA A:885, GLU A:880, PHE A:961, TYR A:867 and LYS A:833.		MET A:953,	LEU A: 963.
TERT(3DU6) 9.11	ARG A:592.		A:591, ARG A:547, GLU A:84., PHE A:417 and ALA A:484			
AKT1(3CQU) 9.37	TYR A:350.		GLY A:680,ASN A:684, VAL A:607, GLU A:675 and THR A:674.		CYS A:677	ARG A:346
VEGFR2(2OH 4) -8.04	TRP A:1094	MET A:1123	THR A:1121 and PRO A:1126			
BCL2(2W3L) 8.83	TRP A:135 and TYR A:139.		GLU A:94 and GLU A:138.			

Table-12. ADME properties

Property	Model name (Unit)	Iso-rhapontigenin	Scutellareintetramethyl ether	Iso-wighteone
Absorption	Water solubilities (Log/mol/L)	-3.817	-4.426	-3.368
	CaCO2 permeabilities (LogPapp in 10^{-6} cm/s)	0.823	1.172	0.876
	Intestinal absorption (%)	93.54	98.35	91.423
	Skin permeability (Log kp)	-2.735	-2.615	-2.737
	P-glycoprotein substrate	Yes	No	Yes
	P-glycoprotein I inhibitor	No	Yes	No
	P-glycoprotein II inhibitor	Yes	Yes	No
Distribution	VDss-human (Log/L/kg)	0.021	-0.112	-0.078
	Fraction unbound-human (Fu)	0	0.168	0.067
	BBB permeability (Log BB)	-0.775	-0.586	-0.817
	CNS permeability (Log Ps)	-1.904	-2.283	-2.277
Metabolis	CYP2D6 substrate	No	No	No
	CYP3A4 substrate	Yes	Yes	Yes
	CYP1A2 inhibitor	Yes	Yes	Yes
	CYP2C19 inhibitor	Yes	Yes	Yes

m	CYP2C9 inhibitor	Yes	No	No
	CYP2D6 inhibitor	No	No	No
	CYP3A4 inhibitor	No	No	No
Excretion	Total clearance (Log/ml/min/kg)	0.193	0.785	0.087
	Renal OCT2 substrate	No	Yes	No
Toxicity	AMES Toxicity	No	No	Yes
	Max. tolerated dose in human (Log/mg/kg/day)	0.542	0.153	0.233
	hERG I inhibitor	No	No	No
	hERG II inhibitor	No	No	No
	Oral Rat Chronic Toxicity (mol/kg)	2.328	2.4	2.285
	Oral Rat Chronic Toxicity (Log/mg/kg_bw/day)	2.175	1.262	0.954
	Hepatotoxicity	No	No	No
	Skin sensitization	No	No	No
	T-Pyriformis toxicity	0.327	0.468	0.75
	Minnow toxicity	1.128	0.465	1.206

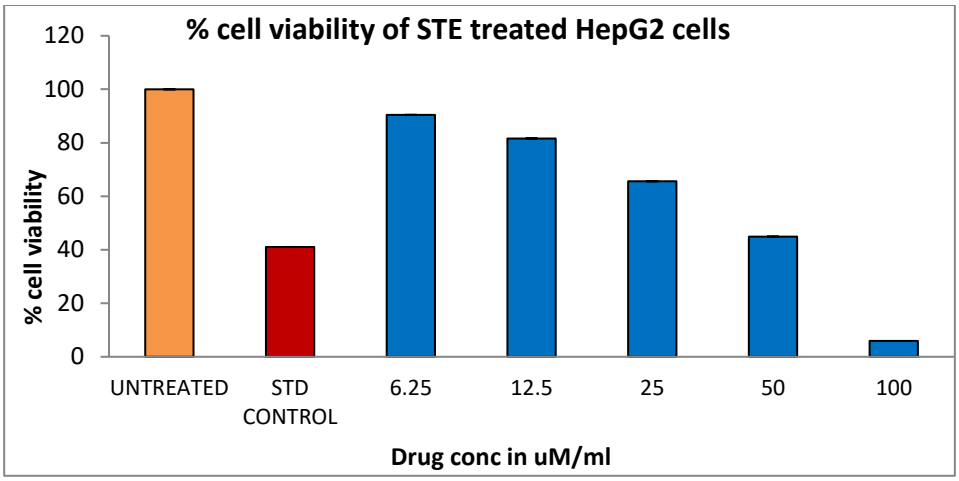

Figure 1: Cell viability(%)values of STE against HepG2 cells post 24hrs

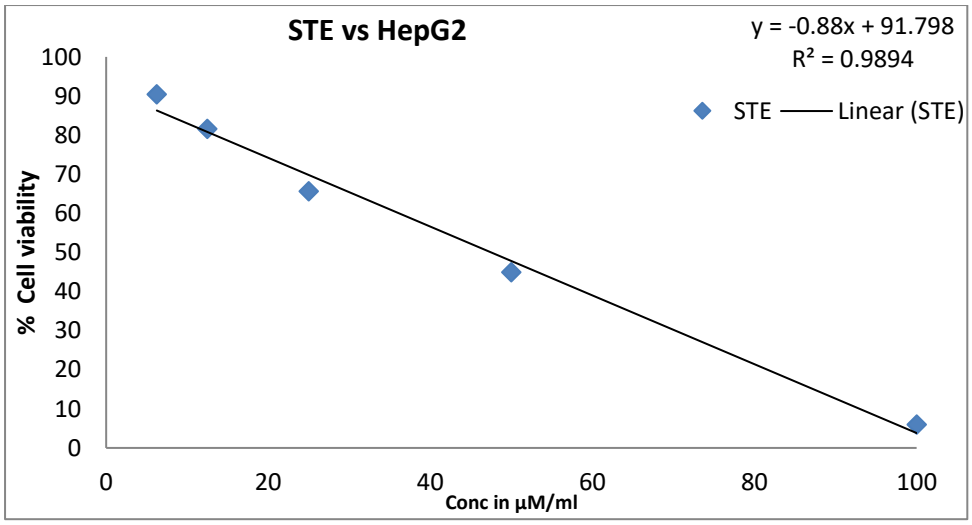

Figure 2: Linear representation of Concentration of STE vs. % Cell viability

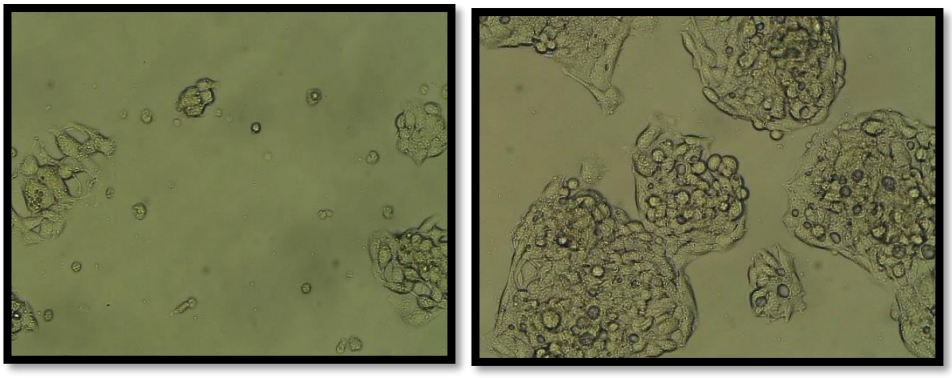

a) HepG2-Untreated b) HepG2-Standard

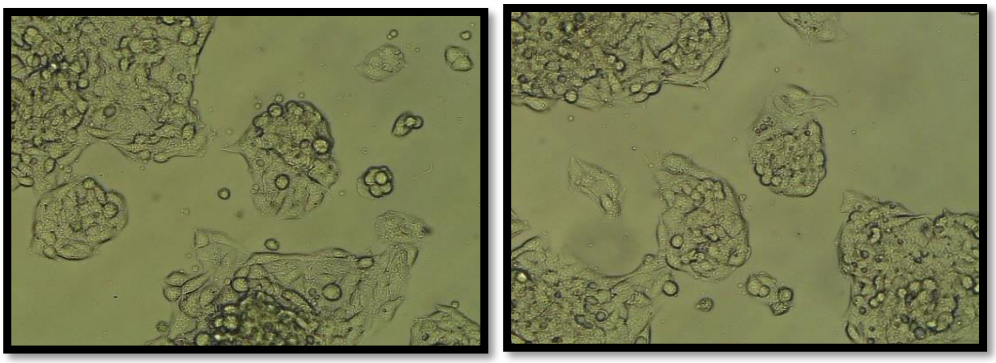

c) STE-6.25µM d) STE-12.5µM

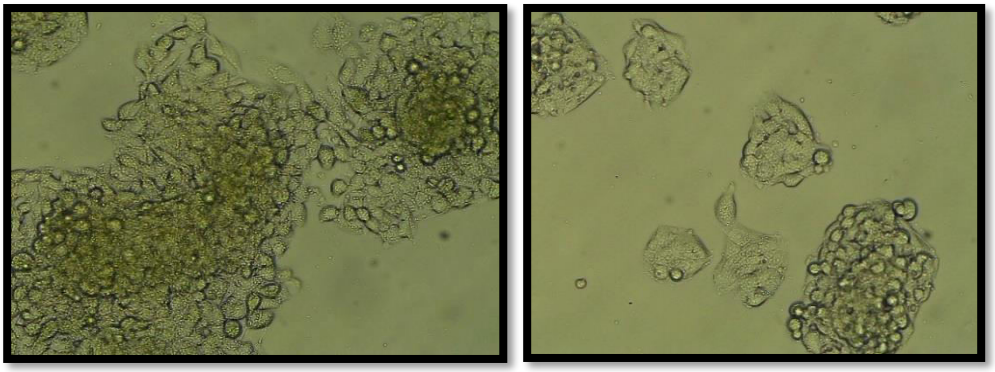

e) STE-25µM f) STE-50µM

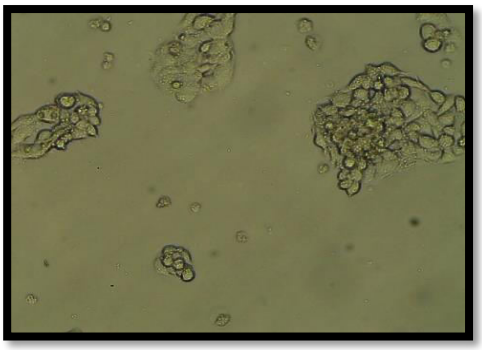

g) STE-100µM

Figure 3: Microscopic images taken post incubation, after the treatment of test compound at different concentrations to HepG2 cells. (a) The untreated HepG2 cells exhibit an epithelial -like morphology and they have high proliferation rates (Clumping). (b) HepG2 cells treated with standard control Doxorubicin (3µM), the shrinkage of cells is observed. (c) HepG2 cells were treated with the concentration of 6.25µM test compound with no visible change in cell mass. (d) HepG2 cells treated with the concentration of 12.5µM test compound with change in the cell mass. (e) HepG2 cells was treated with the concentration of

25µM test compound with shrinkage (f) HepG2 cells was treated with the concentration of 50µM test compound with higher no of cells in shrinkage compared to 25µM concentration. (g) HepG2 cells was treated with the concentration of 100µM test compound with decreased concentration.

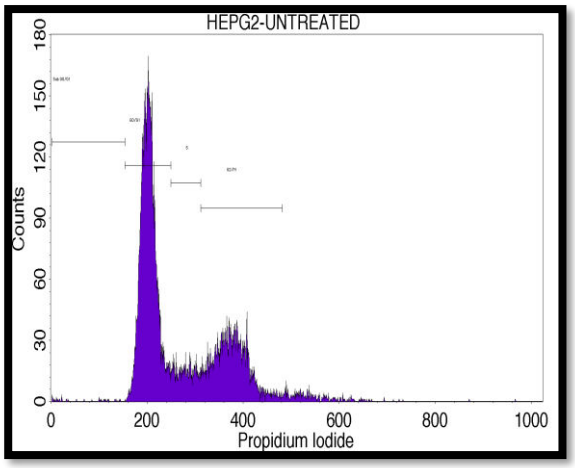

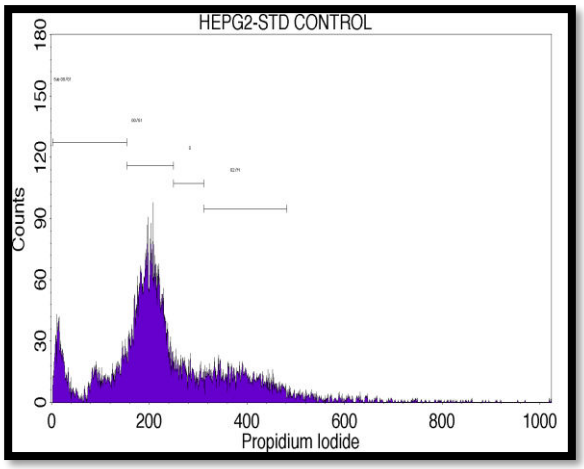

a) Histogram of cell control of HepG2 cells **b) Histogram of HepG2 cells treated Std control**

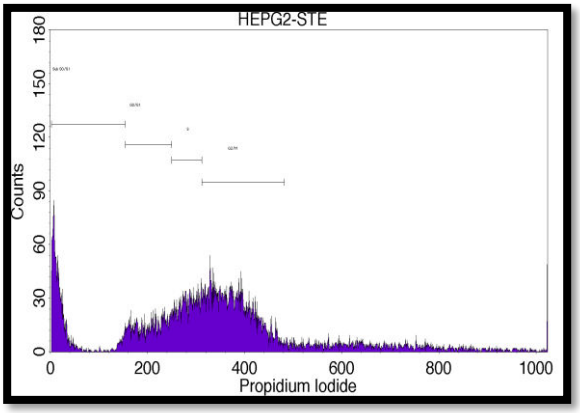

c) Histogram of HepG2 cell treated with STE

Figure 4: Flow cytometry histograms showing the phases of cell cycle distribution in the HepG2 cell line treated with test compound, STE with IC_{50} value and standard drug Doxorubicin at 3µM/ml concentration compared to the control.

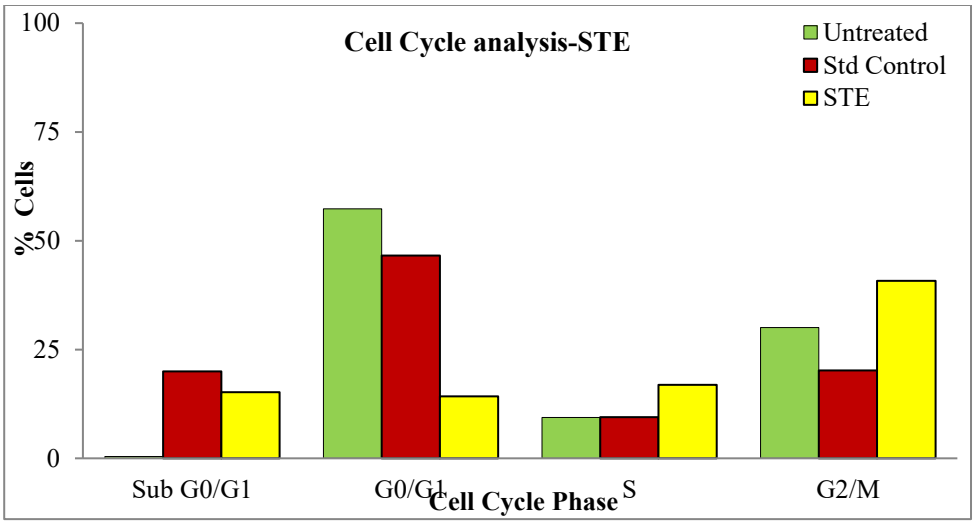

Figure 5: Graph depicting the cells (%) arrested in the different stages of HepG2 cell cycle. The cells treated with test compound with IC_{50} concentration showed high cells (%) at G2/M phase, S phase and Sub G0/G1 phase when compared to Untreated cells. Cell cycle was arrested at G2/M phase, S phase and Sub G0/G1 phase. Doxorubicin was used as a standard control for the study which showed high cells (%) arrested at Sub G0/G1 phase (Apoptotic phase) respectively.

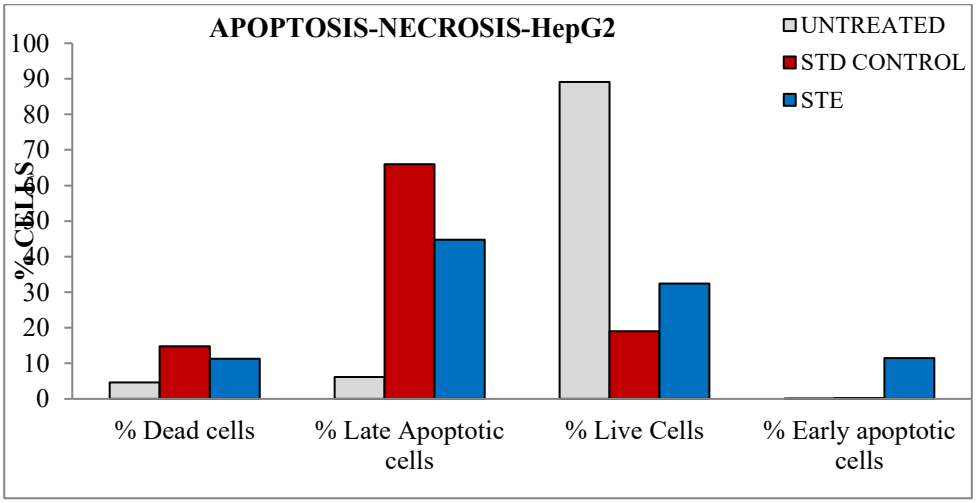

Figure 6: Bar graph depicting the HepG2 live, apoptotic and necrotic cells (%) The number of apoptotic cells was higher in the late stage when compared to the stages.

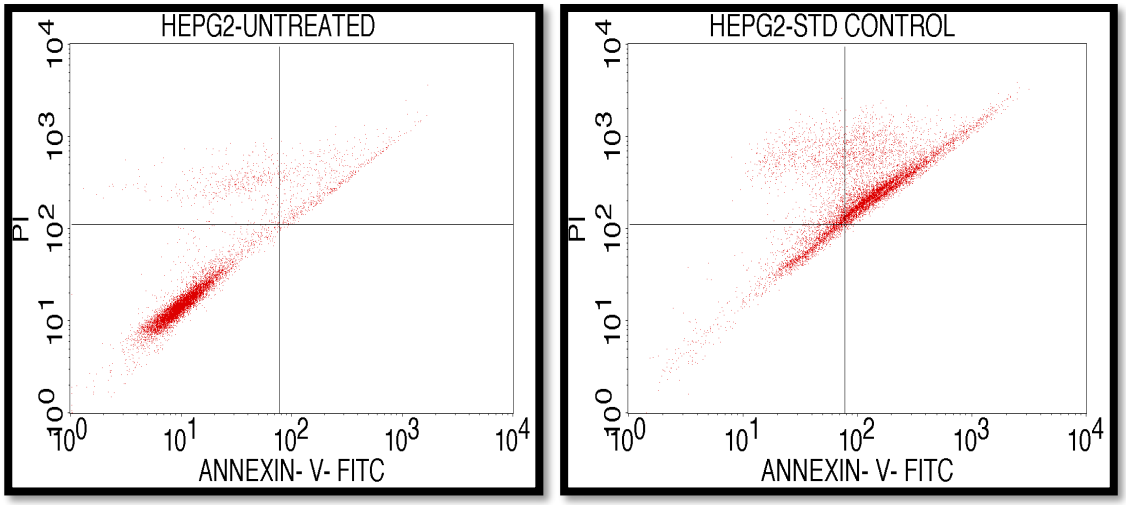

a) HepG2- untreated cells b) HepG2-Std Control

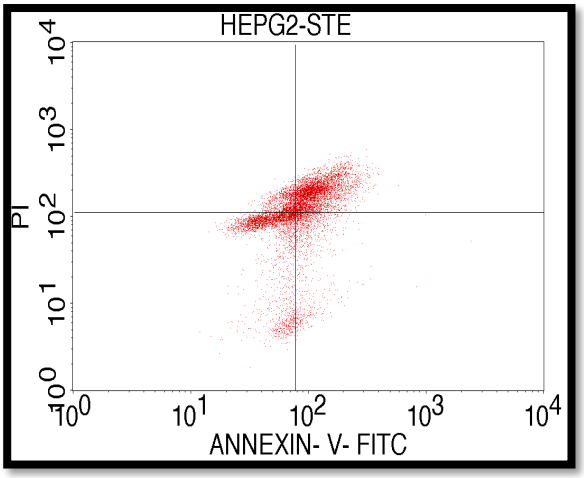

c) HepG2 cells treated with STE

Figure 7: Dot plots of cells distribution due to apoptosis. Quadrant representation: UL – Upper left: % of Necrotic Cells, UR - Upper right: % Late Apoptotic Cells, LL- Lower left: % Viable Cells, LR- Lower right: % of Early apoptotic cells. Annexin V/PI expression in HepG2 cells upon culturing in the presence and absence of test compound-STE with 47.49 µM concentration. Doxorubicin with 3uM concentration was used for the study. Annexin V- FITC was used as Primary Marker, PI- Propidium was used as Iodide Secondary fluorescence Marker.

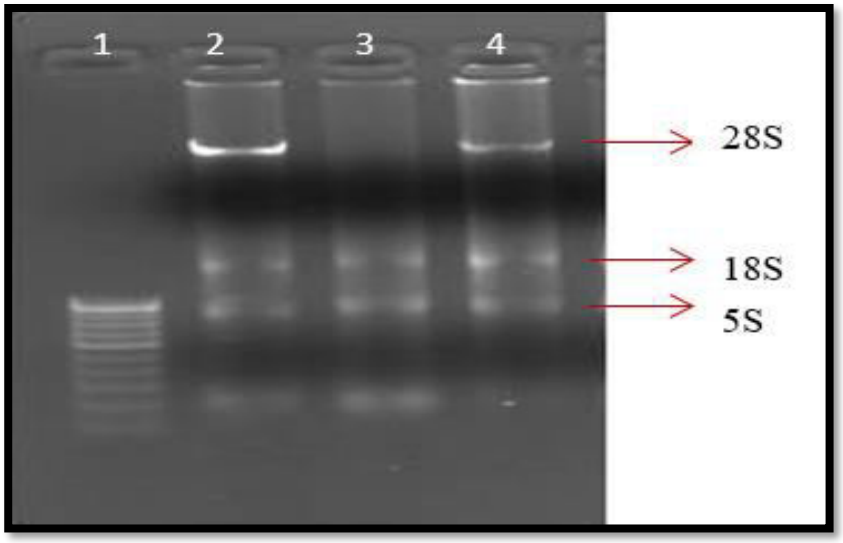

Figure-8: Agarose gel image of Isolated RNA from Untreated, Std control and STE with 47.49µM treated HEPG2cells

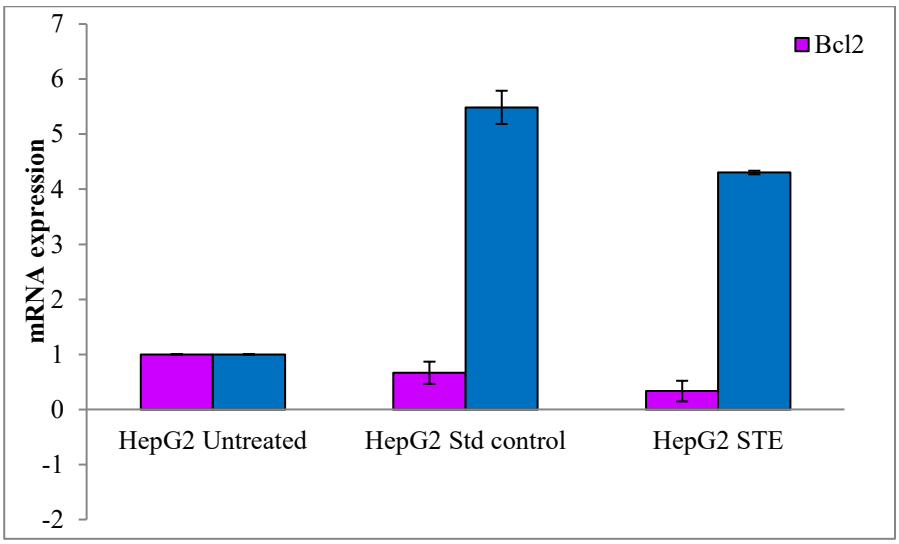

Figure 9: Relative mRNA expression of Caspase-3 and Bcl2 genes in STE treated and non-treated Human hepatocellular adenocarcinoma (HepG2) cells by RT-q PCR. The Bcl2 expression was downregulated by 0.333 folds which is 50% lower when compared to the standard control which has a fold change of 0.666.The gene expression of caspase-3 was upregulated by 4.303 folds which is near to the standard fold change value.

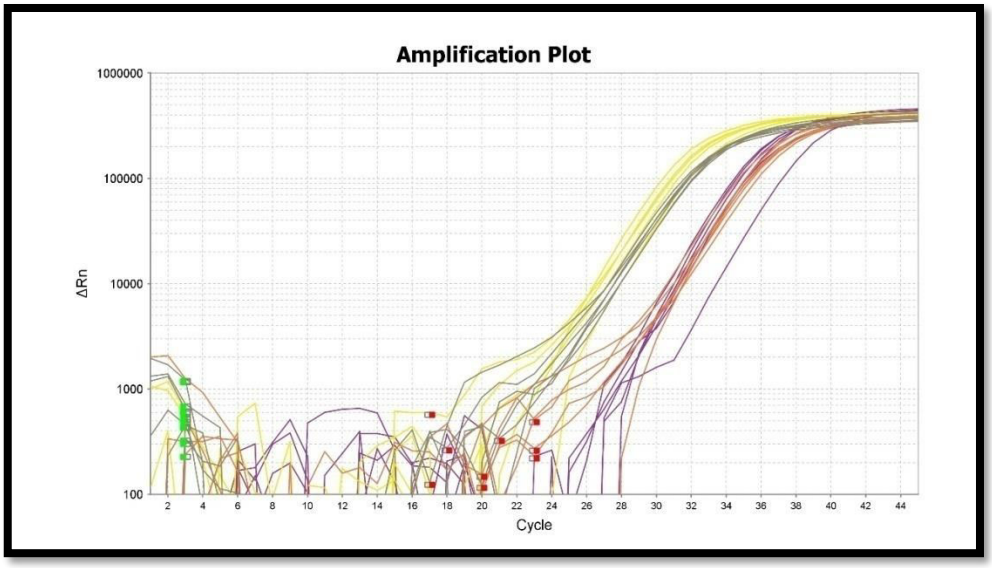

Figure 10: Validation of Bcl2, Caspase-3 and Beta actin primers with each cDNA. The fold expression was calculated with the observed Ct values for each gene with respect to the treated and untreated samples.Caspase-3 gene was up-regulated and BCl2 gene was down regulated in treated groups compared to untreated group. Beta actin was used as internal control in the current study. Yellow curve represent -Caspase 3 expression, Purple curve represents Bcl2 expression and Red curve Represents Beta actin expression.

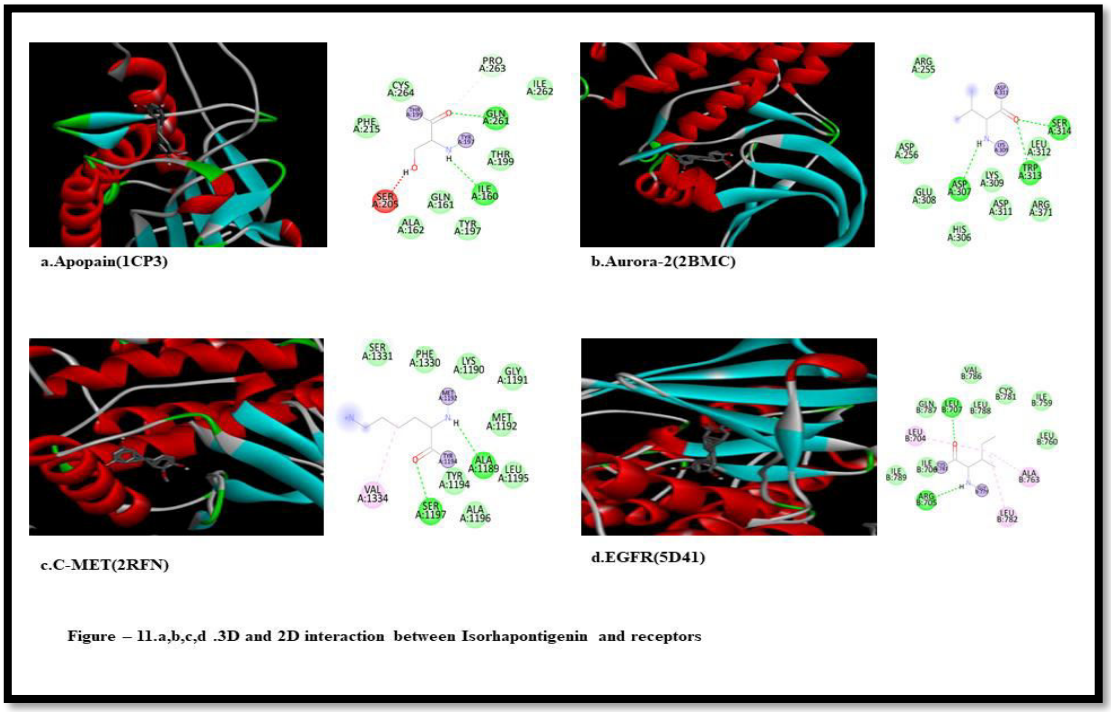

Figure – 11.a,b,c,d .3D and 2D interaction between Isorhapontigenin and receptors

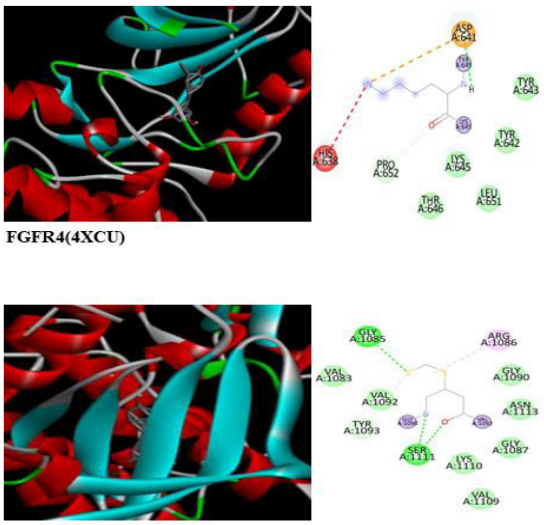

FGFR4(4XCU)

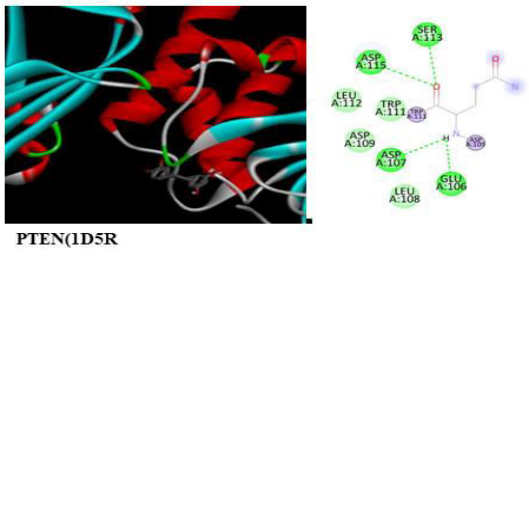

PTEN(1D5R

VEGFR (4MXC)

Figure – 11. e,f , g and 2D interaction between Isorhapontigenin and receptors

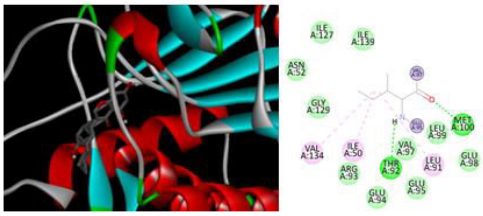

a.Apopain(1CP3)

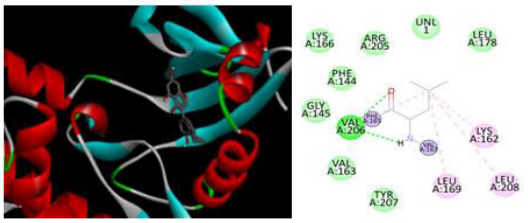

b.Aurora-2(2BMC)

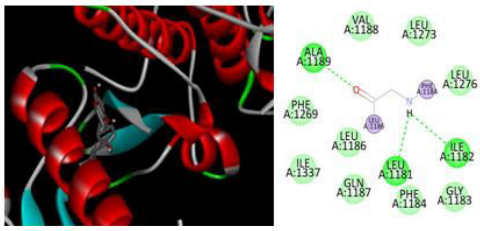

c. C-MET(2RFN)

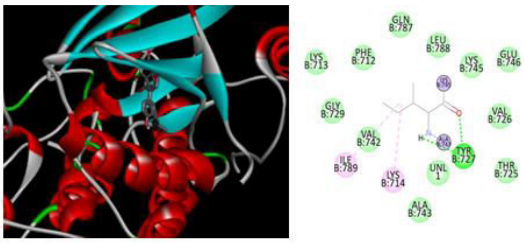

d.EGFR(5D41)

Figure – 12..a,b,c,d .3D and 2D interaction between Isorhapontigenin and receptors

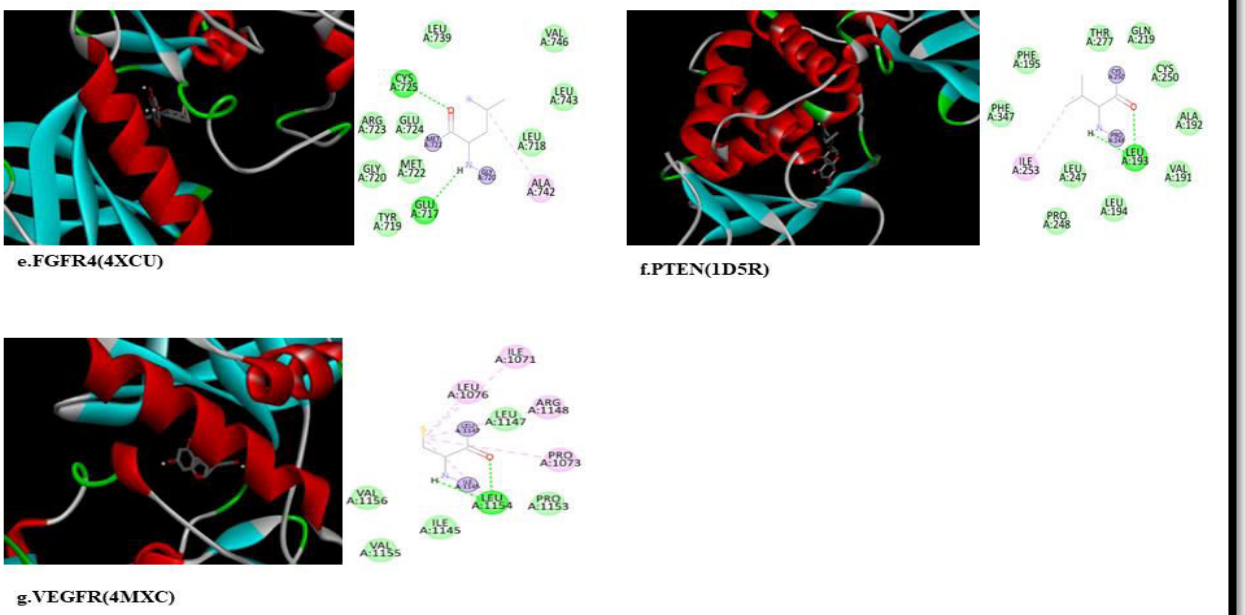

e.FGFR4(4XCU)

f.PTEN(1D5R)

g.VEGFR(4MXC)

Figure – 12.e,f,g,h, .3D and 2D interaction between Isorhapontigenin and receptors

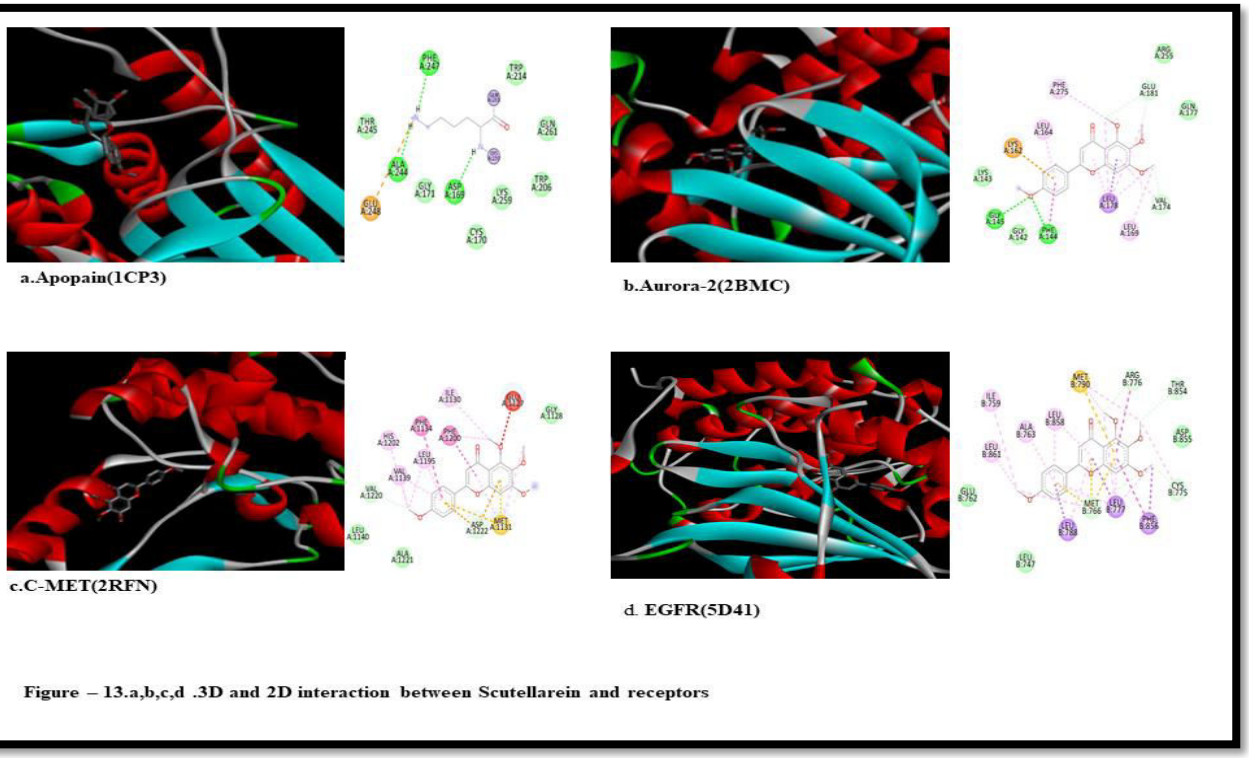

a.Apopain(1CP3)

b.Aurora-2(2BMC)

c.C-MET(2RFN)

d. EGFR(5D41)

Figure – 13.a,b,c,d .3D and 2D interaction between Scutellarein and receptors

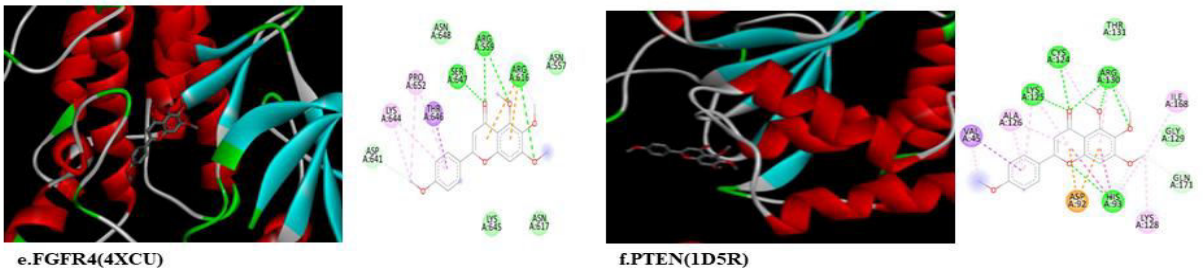

e.FGFR4(4XCU)

f.PTEN(1D5R)

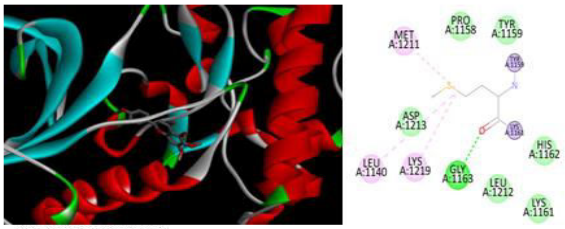

g.VEGFR(4MXC)

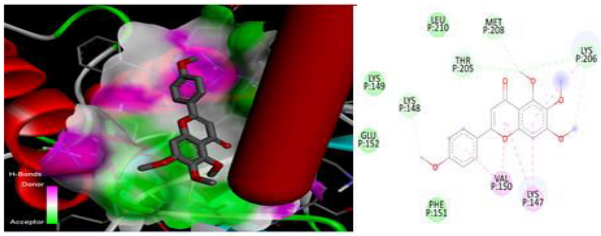

h. NFkB(1SVC)

Figure – 13.e,f,g,h .3D and 2D interaction between Scutellarein and receptors

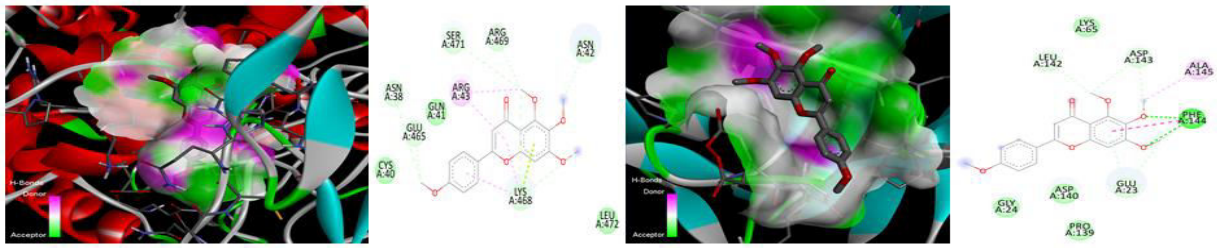

i.Cox2(4FM5)

j.TNF-alpha(6OOY)

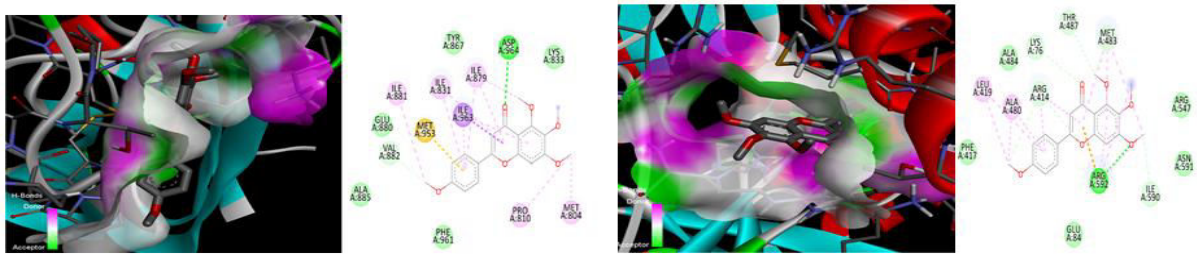

k.PI3K(4FJZ)

l.TERT

Figure – 13.i,j,k,l.3D and 2D interaction between Scutellarein and receptors